



D6.1 Low damage solar cell cutting

Project Information	
Title	From solar energy to fuel: A holistic artificial photosynthesis platform for the production of viable solar fuels
Acronym	REFINE
Project Call	HORIZON-CL5-2022-D3-03
Project Topic	HORIZON-CL5-2022-D3-03-03
Grant Agreement ID	101122323
Project Duration	48 months: 1st November 2023 – 31st October 2027

Document Information	
Contractual Date of Delivery	M15
Actual Date of Delivery	M15
Author(s)	Chang Chuan You, Kristin Bergum, Per-Anders Hansen, Ørnulf Nordseth, and Junjie Zhu
Lead Participant	IFE
Contributing Participant(s)	-
Work Package(s)	WP6
Dissemination Level (PU/SEN)	PU
Nature (R/DEC/DEM/DMP)	R
Version	1.0







Document History

Version	Issue Date	Changes
[1.0]	30.01.2025	



Table of Contents

1	SUMMARY AND SCOPE		
2	INTRODUCTION		
_			
2.1	Main objectives	3	
3	MATERIALS AND METHODS	4	
3.1	LASER SCRIBING AND MECHANICAL CLEAVING FOR THE SOLAR CELL SEPARATION	4	
3.2	EDGE SURFACE PASSIVATION	5	
3.3	Photoluminescence imaging	ε	
4	RESULTS AND DISCUSSION	7	
4.1	INITIAL SURFACE PASSIVATION OF SILICON WAFER SAMPLES	7	
4.2	AFTER CUTTING OF SILICON WAFER SAMPLES	8	
4.3	AFTER HF DIP AND EDGE PASSIVATION		
4.4	EDGE PASSIVATION WITHOUT HF DIP		
4.5	EDGE PASSIVATION OF SMALL CUT TOPCON AND SHJ SOLAR CELLS	10	
5	Conclusions	12	
5.1	Outlook	12	
6	References	12	





1 Summary and scope

In deliverable D6.1, we have developed an in-house edge passivation process that can improve the electrical performance of small-cut solar cells intended to power the REFINE device structure Unit 1. The main highlights are as follows: (i) Effective edge passivation is crucial, especially when the edge-to-bulk ratio becomes large (e.g., small pieces or thin stripes of solar cells); (ii) Mechanically cleaved edges provide the lowest cutting damage after cell separation, and thus a better edge passivation performance can be realized as compared to laser-scribed edges with high damage.

2 Introduction

Currently, half-cut modules are the preferred choice for achieving higher output power with reduced electrical losses. However, cell separation by lasers (Figure 1 (a)) introduces a critical challenge exposing a fresh edge surface that is susceptible to surface recombination losses, as shown in Figure 1 (b). This challenge is especially pronounced in high-efficiency solar cells [1]. It can be seen from Figure 1 (c)-(d) that the power loss increases considerably with decreasing cell size after cutting (or with increasing K, which is defined as the ratio of edge area to the solar cell total area: $K = S_{\text{edge}} / S_{\text{total}}$). Figure 1 (c)-(d) indicates that cutting a high-efficiency silicon heterojunction (SHJ) or a tunnel oxide passivated contact (TOPCon) solar cell into smaller pieces may reduce the power conversion efficiency (PCE) by as much as $\sim 0.5 - 2.5\%$ absolute in 3x3 cm² cells (K = 1.186%).

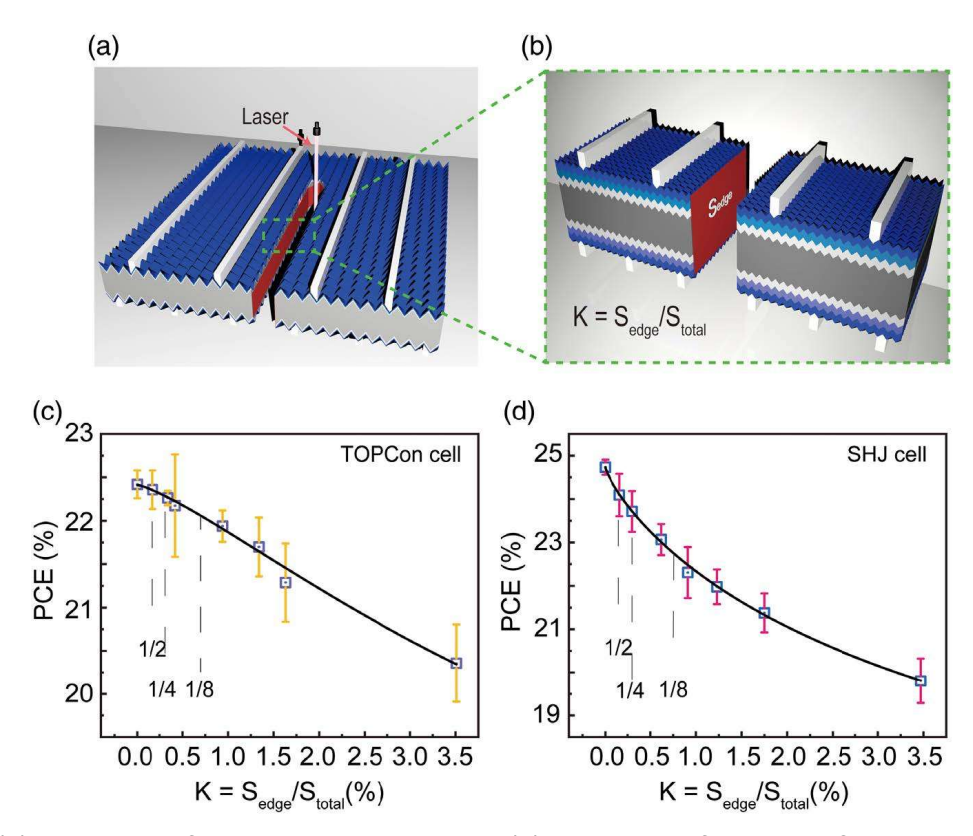


Figure 1: (a) Illustration of the solar cell separation. (b) Illustration of the ratio of edge area to the total area of the solar cell K = S_{edge} / S_{total} . The efficiency loss due to the cutting process for two commercial crystalline silicon cells: (c) TOPCon and (d) SHJ. The images are taken from Ref. [1].

To address the power loss induced by the cell cutting, edge passivation emerges as a promising solution to mitigate these recombination losses and unlock higher efficiencies from cell to module. There are mainly two suggested solutions to recover the efficiency loss caused by the cutting damage: (1)



Atomic Layer Deposition (ALD) for AIO_x layers [2]; and (2) Innovative liquid-based treatments [1, 3]. ALD allows for synthesis of thin films with uniform thickness and excellent surface coverage. Liquid polymer-based solutions can significantly enhance power recovery through edge passivation using Nafion precursor solutions. This method has improved efficiency from 22% to 24.38% in 3x3 cm² SHJ cells [1]. However, stability issues arise when interacting with Polyolefin Elastomer (POE) encapsulants, necessitating a delicate balance between efficiency recovery and compatibility.

Laser scribing and mechanical cleaving (LSMC) is the conventional method for separating the solar cell after the post-metallization and firing stages [2]. However, this cell-cutting technique yields a rough structure at the edge surface, which leads to increased surface recombination. A recent laser cutting process, Thermal Laser Separation (TLS), was developed to address this issue by producing a smoother surface, thereby minimizing power loss and enabling effective passivation with lower surface recombination [1]. By combining TLS with state-of-the-art edge passivation technology based on ALD, recently demonstrated by Fraunhofer ISE [4], a recovery in the energy conversion efficiency (η) of around 0.7% may be attainable, as shown in Figure 2.

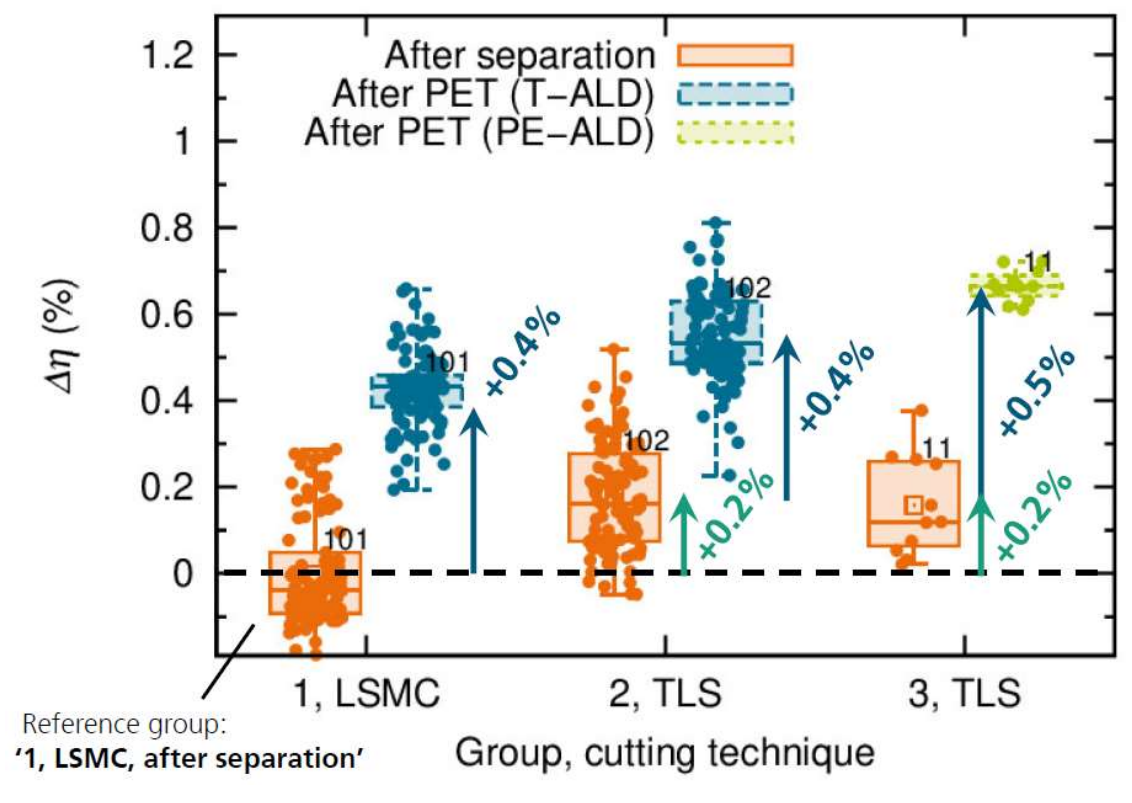


Figure 2: Changes in energy conversion efficiency, Dh, for different groups of laser cutting techniques and passivated edge technologies (thermal and plasma-enhanced ALD). It is shown that an efficiency recovery of 0.7% absolute can be achieved. The image is taken from Ref. [4].

2.1 Main objectives

High-efficiency silicon-based solar cells will be used as the power source for Unit 1. By optimizing the layout of the PV array, the voltage and current can be tailored to meet the necessary conditions for optimal chemical reactions. The lab scale of Unit 1 will be approximately 35 cm², defined by the PV area needed to provide a minimum of 400 mA and 0.72 W at 1.8 V. Therefore, small custom-sized solar cells (dimensions of a few cm) must be created to fit the limited space available.





To deliver the required operating voltage for Unit 1, several small-cut solar cells must be connected. However, the electrical performance, such as cell voltage and current, is compromised due to increased surface recombination at the unpassivated and damaged cut edges if left untreated. Thus, the main goal of this project task is to develop a low-damage cutting procedure for making small solar cells, along with an in-house edge surface passivation process based on plasma-enhanced chemical vapor deposition (PECVD) to minimize PV module power loss.

3 Materials and methods

3.1 Laser scribing and mechanical cleaving for the solar cell separation

Commercial high-efficiency ($\eta \sim 22\%$) bifacial SHJ (160 µm thick) and TOPCon (110 µm thick) solar cells will be used to power Unit 1 in the present project. To optimize the laser scribing/cutting process for separating solar cells, we have used a pulsed picosecond infrared (IR) laser beam with a wavelength of 1030 nm, a frequency of 4 and 10 kHz, a scan speed of 2 mm/s, and various laser powers in an Oxford Lasers system (model J-1030-515-343 FS) with an Amplitude s-Pulse HP laser, Additionally, a pulsed nanosecond Rofin laser (model PowerLine 20E-LP SHG2) with a green laser beam with a wavelength of 532 nm, a frequency of 20 kHz, a diode current of 38 A (i.e., constant laser power), and a scan speed of 100 mm/s was also used. In order to evaluate the edge passivation performance, the laser power and cutting repetitions were varied to obtain cut edges with different degrees of laserinduced damage, in addition to a mechanically cleaved smooth edge without any laser damage. Note that all laser processing was carried out on the rear side of the solar cells. In the left pane of Figure 3. a representative SHJ solar cell sample is shown. This sample was created by first laser-scribing the cell to about one-third of its total thickness along the sample length, followed by mechanical cleaving to separate it. The middle and right panes of Figure 3 display SHJ and TOPCon solar cell samples, respectively, which were obtained by first using a diamond scribe to mark the surface of the cell along a desired cleave plane, and then mechanically cleaving the cells along this line, avoiding any laser damage. Note that, unlike the laser-scribed cell shown in the left pane in Figure 3, the busbars and metal fingers of the mechanically cleaved cells (the middle and right panes in Figure 3) are oriented at approximately 45° to the cut edges. This is due to the silicon wafer's (100) crystal orientation, which results in a cleave plane in the [110] direction. The small solar cell samples measure about 2x2 cm².



Figure 3: Left pane: Laser-scribed and mechanically cleaved SHJ solar cell. Middle pane: Mechanically cleaved SHJ solar cell using a diamond scribe. Right pane: Mechanically cleaved TOPCon solar cell using a diamond scribe. The cell size is about 2x2 cm².

SEM imaging was employed to examine the quality of the different cut-edge surfaces using a JEOL JSM-7900F field-emission scanning electron microscope. Figure 4 shows SEM cross-section images of cut edges with various degrees of damage and can be divided into four categories:

- 1. Mechanically cleaved edge using a diamond scribe with **no laser damage** (Figure 4 (a))
- 2. Laser-scribed (approximately one-third of the total cell thickness) and mechanically cleaved edge with **low laser damage** (Figure 4 (b))



- 3. Laser-scribed (approximately two-thirds of the total cell thickness) and mechanically cleaved edge with **moderate laser damage** (Figure 4 (c))
- 4. Laser-cut edge (i.e., completely cut through the cell) with high laser damage (Figure 4 (d))

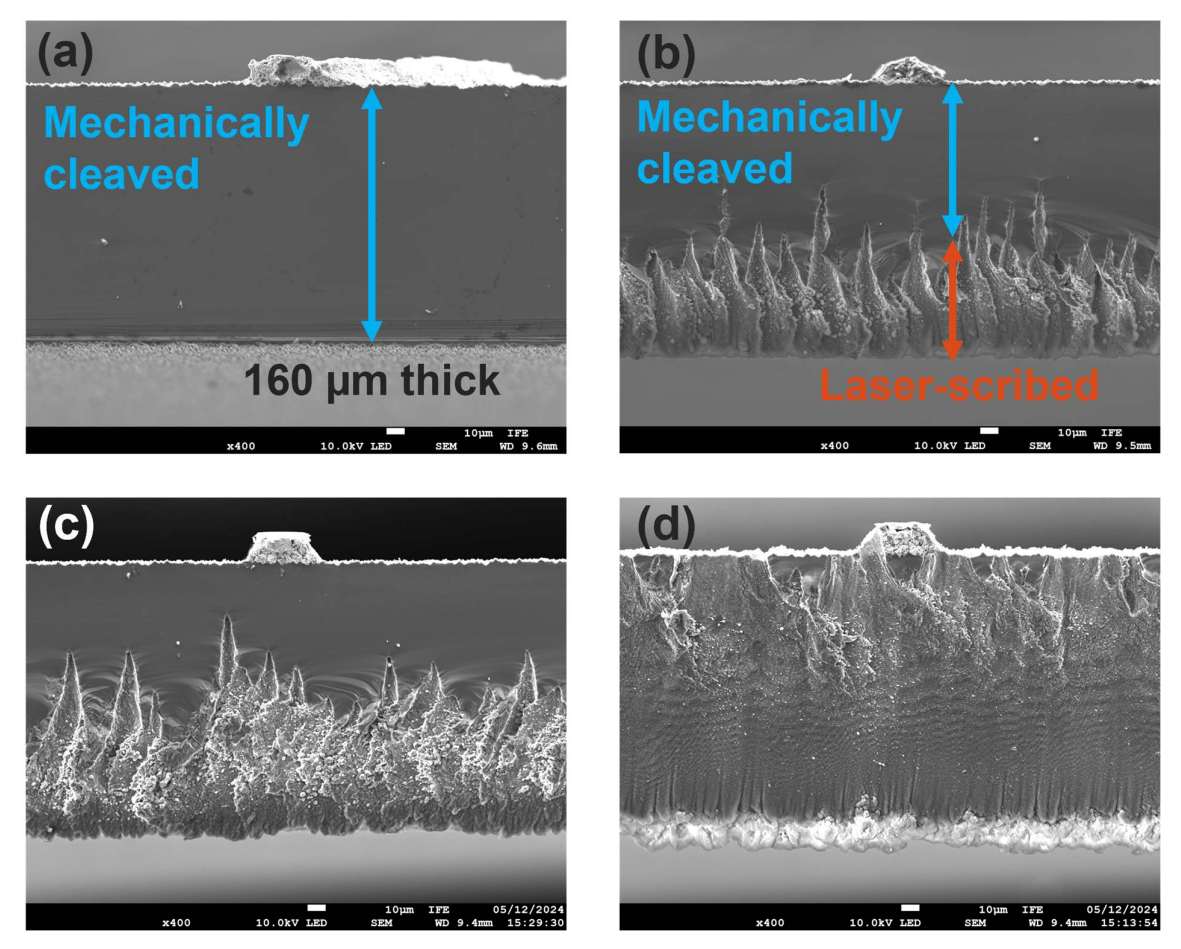


Figure 4: SEM cross-section images of (a) a mechanically cleaved cell edge, and laser scribed and mechanically cleaved cut edge with (b) low laser-induced damage, (c) moderate laser damage, and (d) high laser damage.

For the edge surface passivation experiments, small pieces were cut (with different cut edge damages) from a 4-inch planarized (by chemical mechanical polishing), (100)-oriented, n-type FZ monocrystalline silicon wafer from TOPSIL, in addition to small-cut solar cells. The silicon samples were included to investigate the passivation in a simpler structure. Additionally, the TOPSIL silicon wafer (280 μ m thick) is thicker than the solar cells, leading to a larger edge area.

3.2 Edge surface passivation

Edge passivation of small cut cells provides both some challenges and opportunities. The small sample size makes them difficult to handle, but also allows vertical stacking which would not be possible with larger pieces or full wafers. Several different sample preparations and stackings were therefore explored. Figure 5 shows three different sample stackings for edge passivation with PECVD. The red area is the coated surfaces, blue wafers are the cell samples and grey wafers are dummy wafers used to control and avoid deposition on other surfaces than the edges. Stacking A and B will allow coating on only the edge surface while avoiding the cell's front and back faces. Stacking C will also have a coating on one of the cell's faces. In the units we are constructing in REFINE, coating the backside of



the cell is not very problematic. For stacking B, it proved challenging to get the sample and covering wafer to be the exact same dimensions, and to align them perfectly by hand. Thus, stacking C is a reasonable approach in this project.

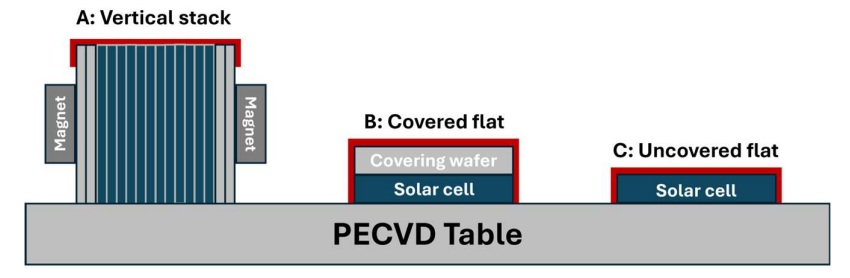


Figure 5: Illustration of three different sample stacking methods used. Blue wafers are cell sample pieces, grey wafers are dummy wafers used to prevent deposition onto the cell's faces, and red is the deposited passivation coating.

The passivation chemistry utilized is a stack of hydrogenated amorphous silicon (a-Si) and silicon nitride (SiN_x) that provides high-quality surface passivation. The top SiN_x layer also acts as a capping layer to minimize the potential damage to the underlying a-Si layer during sample handling and measurement. These layers are deposited by PECVD at 230 °C. Figure 6 shows a vertical stack just after cleaving and after deposition of the SiN_x/a -Si stack. The PECVD coating covers some distance down the sides of the stack. The stack can be turned around to coat the other long edge. But as can be seen, the short edges will be partially and unevenly double-coated. The simplest and most applicable stacking was type C, lying flat with no cover.

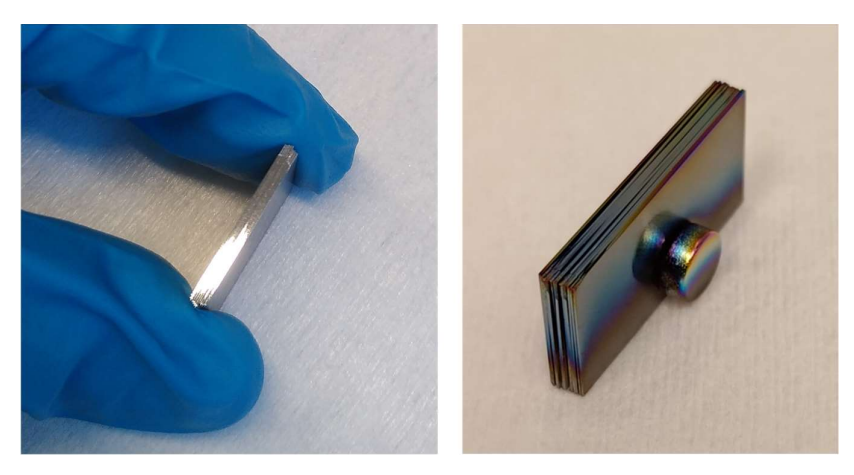


Figure 6: Photos of a vertical stack of cell samples sandwiched between grey dummy wafers, cleaved edge facing upwards. It is not possible to distinguish the cells in the stack as the cleaved edges align well.

3.3 Photoluminescence imaging

Photoluminescence imaging (PLI) was done in an BT Imaging LIS-R1 unit, using a high-magnification lens. In PLI, wafer areas with good surface passivation show high photoluminescence (PL) intensity. As electron-hole pairs are generated in the wafer bulk, they can move around and will eventually recombine either radiatively emitting a photon, or non-radiatively. Surface passivation aims to remove as many as possible of the non-radiative recombination pathways at the wafer surfaces, which otherwise is the major recombination pathway. A laser-damaged cut edge will be a surface with a very





high density of non-radiative recombination sites and will effectively reduce the effective lifetime of carriers within the carrier diffusion length of this surface. In PLI, the wafer will show decreasing PL intensity towards the edge. If the edge has few recombination sites (as in a cleaved edge) and is well passivated, the PL intensity will continue to be high much closer to the edge. Thus, good edge passivation can be seen in PLI as a steep increase in PL intensity from the edge toward the bulk, while poor edges will show low PL intensity further toward the bulk. Note that the PL intensity is a direct measure of the surface passivation quality. A high PL intensity indicates low cutting damage, which in turn allows for achieving a high operating cell voltage.



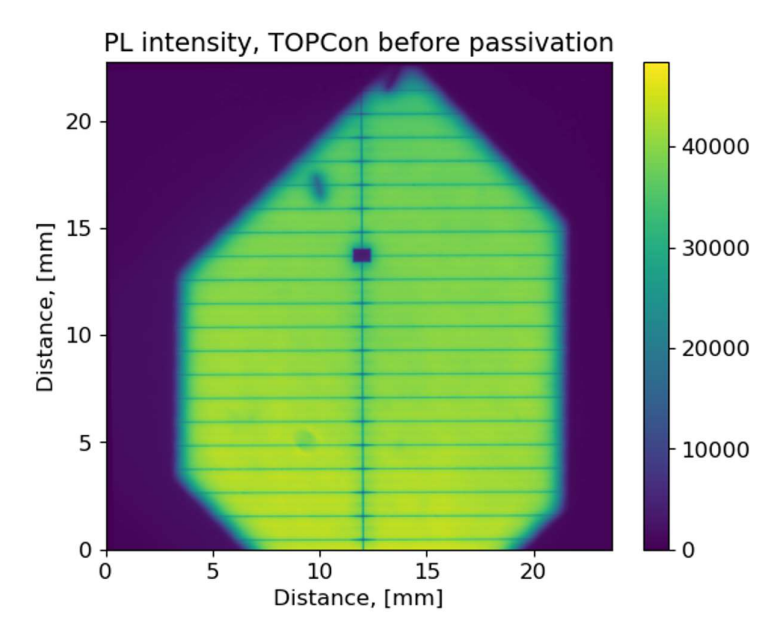


Figure 7: A representative PL image (right pane) of a TOPCon solar cell cut into a small shape (left pane), showing high PL intensity from the bulk of the cell which decreases to zero at the edges. Metal fingers are also clearly visible, and any scratches that have damaged the passivation coating show up as pixels with low PL intensity.

4 Results and discussion

4.1 Initial surface passivation of silicon wafer samples

The initial surface passivation was performed on silicon wafer samples containing both a cleaved edge and a laser-cut edge with high damage. The effective minority carrier lifetime of the passivated silicon wafer sample was measured at ~ 5 ms at a carrier injection level $\Delta n = 1 \times 10^{15}$ cm⁻³. PLI was performed after the initial passivation process to investigate the differences between the passivation of the two types of edges. As can be seen in Figure 8 (a), the edge of the cleaved sample appears sharp in the image, whereas the laser-cut edge in Figure 8 (b) is diffuse. The PL intensities were then averaged across the area shown, and the resulting comparison between these two averaged intensities is plotted in Figure 8 (c). Note that the chosen area represents the best cases for the samples, as areas with visible artifacts not related to edge passivation, were discarded. In the averaged plot, it is clear that the passivated cleaved edge has an initial steep slope in PL intensity at the edge of the sample. After the steep incline, the slope changes markedly and becomes similar to that seen in the laser-cut sample. For the laser-cut sample, there is a more gradual increase in PL intensity, with very little intensity close to the edge of the sample.



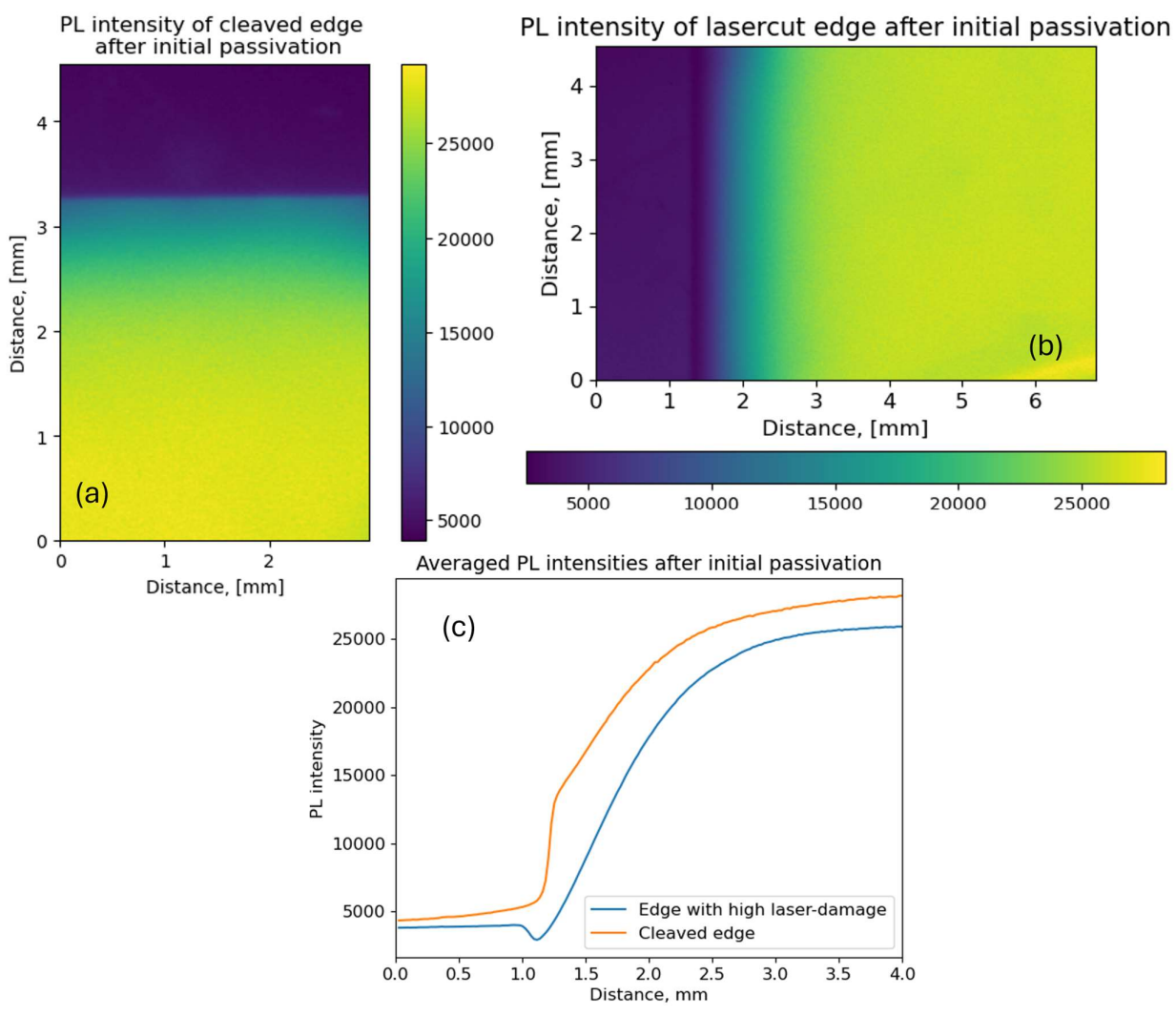


Figure 8: PL image of (a) a cleaved edge and (b) an edge with high laser damage after the silicon wafer sample was passivated (SiN_x/a-Si stack) on both sides. (c) A comparison of averaged PL intensities of the two edges.

4.2 After cutting of silicon wafer samples

The passivated silicon wafer samples were then cut into smaller pieces. Three different edges were created; cleaved without laser damage, mild (low) laser damage, and high laser damage. Averaged PL intensities of these samples are found in Figure 9. None of these edges show the initial steep slope after cutting, as expected with exposed surface on the side but the gradual slope as seen for highly laser-damaged edge. There appears to be nearly no difference between the three different edges.





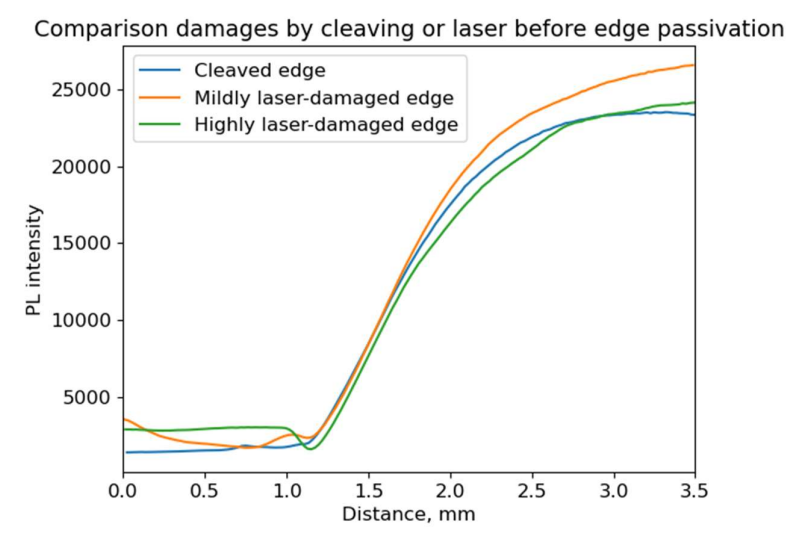


Figure 9: A comparison of three different (non-passivated) edges after cleaving and laser-cutting a passivated silicon wafer sample.

4.3 After HF dip and edge passivation

One silicon wafer sample containing all three types of edges was dipped in hydrofluoric (HF) acid (5% in DI water) for 10 seconds, followed by rinsing in DI water, blow-drying with a nitrogen gun, and immediate insertion into the PECVD vacuum chamber to avoid surface oxidation. Note that this treatment removed the SiN_x layer on top of the wafer, and thus impacted the total PL intensity in the PLI. Subsequently, the SiN_x /a-Si passivation stack was deposited on one side of the sample (backside) only. The PL images were obtained from the front side of the sample. PL images from both before and after edge passivation can be seen in Figure 10.

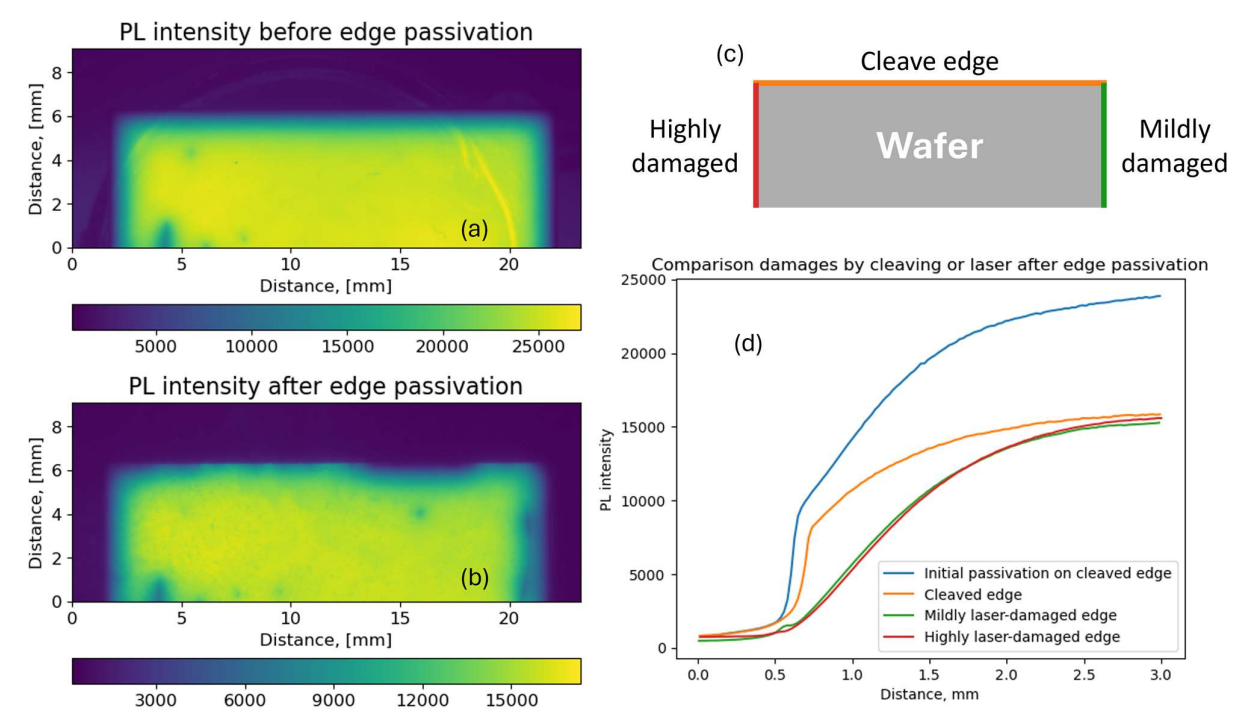


Figure 10: PL images of a passivated wafer (a) before edge passivation and (b) after edge passivation. The top edge shows the cleaved edge, the left edge has high laser damage, whereas the right edge





has mild laser damage, as illustrated in (c). Averaged PL intensity over these edges is shown and compared in (d). Note that the initial passivation graph was shifted down by 4000 counts for better comparison.

The PL images show the same sample, before and after HF dip and edge passivation. The top edge shows the cleaved edge, the left edge is highly laser-damaged, whereas the right edge is mildly laser-damaged. While there appears to be no change in the sharpness of the laser-damaged edges, the cleaved edge shows an increase in sharpness in some areas. Averages of best-case areas were extracted and are shown in Figure 10 (d). The passivated cleaved edge shows a similar shape as was obtained for the initial passivation (Figure 8 (c)), with an initial steep slope at the edge, suggesting that the edge passivation was successful.

4.4 Edge passivation without HF dip

The edge passivation was also performed on samples that were not dipped in HF before deposition. These showed no distinguishable improvement upon edge passivation, compared to non-passivated edges.

4.5 Edge passivation of small cut TOPCon and SHJ solar cells

Small TOPCon and SHJ solar cell test samples with three different edges were investigated: cleaved edges, mildly laser-damaged edges, and highly laser-damaged edges. The edge passivation stack was deposited directly on the samples without HF dip, as this would damage the solar cells.

The PL intensity is reduced due to the front metal fingers. As a result, small sections were extracted from multiple areas before data was averaged. An overview of where the sections were extracted can be found in Figure 11. A comparison of the averaged PL intensities shows that there appears to be no difference in the slope before or after passivation. This could be caused by the edges not being cleaned/etched by HF dip prior to edge passivation or that the thickness of the solar cells is much thinner than that of the silicon wafer samples, making it more challenging to measure the effect of the edge passivation. The dip in the PL intensity curve for the cleaved edge sample in Figure 11 (e) - (f) can be attributed to the reduction in PL intensities due to the metal fingers.



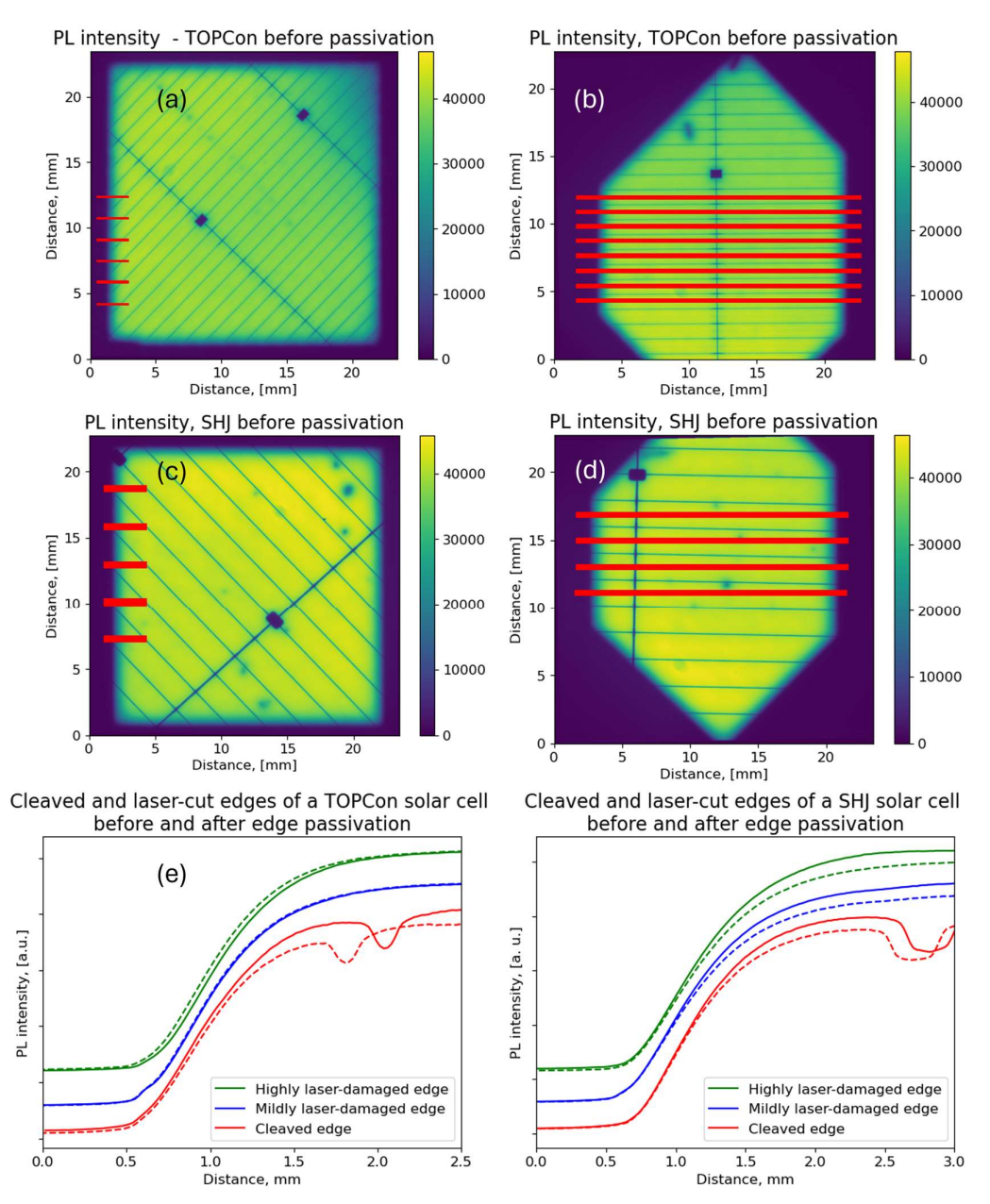


Figure 11: (a) PL image of a cleaved TOPCon solar cell. The red stripes show areas used to extract the average intensities of the cleaved edge. (b) PL image of a TOPCon solar cell which has both cleaved and laser-cut edges. The red stripes show areas used to extract the average intensities of the highly laser-damaged edge (left) and the mildly laser-damaged edge (right). (c) PL image of a cleaved SHJ solar cell. The red stripes show areas used to extract the average intensities of the cleaved edge. (d) PL image of a SHJ solar cell which has both cleaved and laser-cut edges. The red stripes show areas used to extract the average intensities of the highly laser-damaged edge (left) and the mildly laser-damaged edge (right). The extracted average intensities of (e) TOPCon and (f) SHJ edges before and after edge passivation show no discernible changes in the slope. The solid lines show data before edge passivation, whereas the dotted lines show data after edge passivation. The three edges have been shifted along the y-axis to enhance the visibility of the differences before and after passivation.





5 Conclusions

When working with small-cut solar cells in the REFINE device structure, passivation of the edges becomes important when the edge-to-bulk ratio is large (i.e. small pieces or thin stripes). In this work, both mechanically cleaved edges and laser-scribed edges were investigated. Our results show that the mechanically cleaved edge of a silicon wafer can be passivated by PECVD. However, the processing steps are important for successful edge passivation. Successful edge passivation was only observed for wafers that got an HF dip after mechanical cleaving and before passivation. Thus, it seems that a chemical etch treatment or cleaning of the wafer edge after cleaving is required. Moreover, neither mechanically cleaved nor laser-scribed edges of solar cells showed any passivation improvements without a post-cut chemical etch treatment. The solar cells could not be HF dipped in the same manner as the wafers as the HF will likely cause damage to one or more of the materials in the solar cell structure. A post-cut chemical etch treatment of the edge that is compatible with the solar cell structure is required.

5.1 Outlook

Further work is needed to identify the causes preventing proper edge passivation, including developing a post-cleave chemical cleaning process that doesn't affect the rest of the cell (i.e. metal contacts, anti-reflection coating, etc.). When the necessary processes have been developed, the cleaving and edge passivation procedures can be updated, and edge-passivated small-cut solar cells can be delivered to the REFINE device structure.

6 References

- [1] Li et al., Advanced Energy and Sustainability Research, 4 (2023) 2200154.
- [2] Baliozian et al., IEEE Journal of Photovoltaics, 10 (2020) 390.
- [3] Chen et al., Solar Energy Materials and Solar Cells, 258 (2023) 112401.
- [4] Lohmüller et al., PV Magazine Webinar 2023.

Disclaimer

"Funded by the European Union. Views and opinions expressed are however those of the author(s) only and do not necessarily reflect those of the European Union. Neither the European Union nor the granting authority can be held responsible for them."